Supplementary Information

A direct solvent-free conversion approach to prepare mixed-metal metal-organic frameworks from doped metal oxides

Beili Yi,[a] Haojie Zhao,[a] Yue Zhang,[a] Xiaomeng Si,[a] Guanqun Zhang,[a] Yuanyuan An,[a] Longxing Su,[a] Chia-Kuang Tsung [b], Lien-Yang Chou, *[a] and Jin Xie* [a]

[a] School of Physical Science and Technology, ShanghaiTech University, Shanghai 201210, China.

[b]Department of Chemistry, Merkert Chemistry Center, Boston College, Chestnut Hill, Massachusetts 02467, United States.

*xiejin@shanghaitech.edu.cn; zhuoly@shanghaitech.edu.cn

This PDF file includes:

Methods

Materials. Zinc acetate dihydrate ($Zn(OAc)_2 \cdot 2H_2O$, Aladdin, 99%), sodium hydroxide (NaOH, Sinopharm, 96%), hydrogen hexachloroplatinate (IV) hydrate ($H_2PtCl_6 \cdot 6H_2O$ Adamas, 99.95%), dipotassium tetrachloroplatinate (K_2PtCl_4, Adamas, 98%), polyvinylpyrrolidone (PVP, Aladdin), ethylene glycol (Aladdin, 99%), cobalt (II) acetate tetrahydrate ($Co(OAc)_2 \cdot 4H_2O$, J&K, 99.5%), nickel(II) acetate tetrahydrate ($Ni(OAc)_2 \cdot 4H_2O$, J&K, 99%), copper(II) acetate monohydrate ($Cu(OAc)_2 \cdot H_2O$ Acros, 98%), commercial platinum dioxide (PtO_2, Energy Chemical, 99.95%), trioctylamine (Aladdin, 95%), 2-methylimidazole (MeImH, Aladdin, 98%), 2-ethylimidazole (Alfa Aesar, 98%), benzimidazole (TCL, 98%), ethanol (Greagent, 99.7%), acetone (Greagent, 99.5%), hexane (Greagent, 97%), methanol (Greagent, 99.5%), commercial ZIF-8 (Merck), ethylene glycol (Sinopharm, 99%). All materials were used as received without further purification.

Synthesis of ZnO, and Pt-doped ZnO (Pt-ZnO). NaOH (400 mg, 10 mmol) was dissolved in 44 ml deionized water in a three-neck flask and then heated to 110 ℃. After reflux condensation, $Zn(OAc)_2 \cdot 2H_2O$ (1097.5 mg, 5 mmol) dissolved in 6 ml deionized water was added. The solution was kept stirring at 110 ℃ for 30 minutes and then cooled down to room temperature. The solid product was collected by centrifuging at 6000 rpm for 5 minutes. The product (ZnO NPs) was then washed by deionized water twice and dried at 80 ℃ overnight. Pt-ZnO NPs were prepared using the same procedure with the addition of $H_2PtCl_6 \cdot 6H_2O$ (41.5 mg, 0.08 mmol).

Preparation of Pt NPs and ZnO mixture. 0.5 M PVP and 0.01 M $H_2PtCl_6 \cdot 6H_2O$ were dissolved by stirring in 4.25 ml ethylene glycol under N_2 flow at 200 ℃. Then, 0.5 M tetramethyl ammonium bromide in 0.75 ml ethylene glycol was added. After stirring under N_2 flow at 200 ℃ for 20 minutes, the product was washed by an ethanol-acetone mixture for 1 time and an ethanol-hexane mixture for 3 times, respectively. Then the as-obtained Pt NPs were dispersed in 5 ml methanol. Finally, Pt NPs and ZnO NPs were dispersed in methanol by ultrasonication. Physical mixture of Pt NPs on ZnO powder (Pt NPs + ZnO) could be obtained after drying at 80 ℃.

Synthesis of M-ZnO (M = Co, Cu, or Ni). The typical synthesis procedure for M-ZnO in this work was modified based on a previous report[35]. Briefly, a mixture of $Zn(OAc)_2 \cdot 2H_2O$ (2.66 mmol), $Co(OAc)_2 \cdot 4H_2O$ (0.13 mmol, 0.05 equiv), and 25 ml trioctylamine were rapidly heated to 310 ℃ under reflux. The reaction was continued for 45 minutes under stirring and then cooled to room temperature. The sample was washed by methanol twice, centrifuged at 6000 rpm for 5 minutes, and dried at 80 ℃ overnight. Cu-ZnO and Ni-ZnO could be synthesized by replacing $Co(OAc)_2 \cdot 4H_2O$ with $Cu(OAc)_2 \cdot H_2O$ and $Ni(OAc)_2 \cdot 4H_2O$, respectively.

Synthesis of M-ZIF-8 by CVD (M = Pt, Co, Cu, or Ni). In a typical CVD synthesis, 102 mg MeImH was heated to 140 ℃ to generate enough precursor vapor to react with 20 mg Pt-ZnO NPs. After the reaction, samples (labeled as Pt-ZIF-8) were washed by methanol twice, centrifuged at 6000 rpm for 5 minutes, and dried at 80 ℃ overnight. The conversion efficiency can be controlled by carefully tuning reaction time, temperature, and ratio of starting materials. ZnO NPs with different metal ions as dopants (Co, Cu, and Ni) could be converted to M-ZIF-8 using similar CVD approaches.

Synthesis of Pt-ZIF through the solvent-free approach. In a typical solvent-free synthesis, 1.25 mmol 2-ethylimidazole and 40 mg Pt-ZnO was kept at 80 ℃ for 2 d. The product (Pt-MAF-6) was washed by methanol twice, centrifuged at 6000 rpm for 5 minutes, and dried at 80 ℃ overnight. Pt-MAF-6 and Pt-ZIF-7-III were synthesized using a similar solvent-free approach by changing organic linkers and reaction temperatures (140 ℃).

Synthesis of Pt-ZnO@ZIF-8 by solvothermal transformation approach (Pt/ZIF-8-ST). In a typical ST produce, 32 ml ethanol with 50 mg Pt-ZnO and 500 mg MeImH was kept stirring for 2 days at 50 ℃. After the reaction, samples were washed by ethanol twice, centrifuged at 6000 rpm for 5 minutes, and dried at 80 ℃ overnight. The Pt/ZIF-8-ST-1 d and Pt/ZIF-8-ST-4 d can be synthesized by changing reaction time to 1 day and 4 days, respectively.

Synthesis of Pt/ZIF-8 by one-pot reaction approach (Pt/ZIF-8-OPR). 4 ml deionized water with 1.32 g MeImH was added into 10 ml deionized water containing 137 mg $Zn(OAc)_2 \cdot 2H_2O$ and 4.26 mg K_2PtCl_4. After reacted for 3 hours under stirring

(500 rpm) at room temperature, the solution was centrifuged at 12000 rpm for 10 minutes, and then washed with deionized water and methanol, respectively. The product was obtained after drying at 80 ℃ overnight.

Synthesis of Pt/ZIF-8 by post-synthetic exchange approach (Pt/ZIF-8-PSE). 142 mg ZIF-8 and 4.26 mg K_2PtCl_4 were added into 10 ml deionized water. The mixture was stirred for 24 h at room temperature. The mixture was centrifuged at 12000 rpm for 10 minutes and washed by deionized water and methanol. The product was obtained after drying at 80 ℃ overnight.

Characterization

Powder X-ray diffraction patterns (PXRD) were acquired on a Bruker D8 Advance diffractometer with Cu Kα radiation (λ = 1.5418 Å) at 40 kV and 40 mA. Ultraviolet-Visible (UV-Vis) spectra were acquired with a Cary 5000 UV-Vis near-infrared spectrometer. X-ray photoelectron spectroscopy (XPS) spectra were collected on an ESCALAB 250Xi X-ray photoelectron spectrometer. Inductively coupled plasma atomic emission spectroscopy (ICP-OES) data of the samples were collected on an iCAP 7400 inductively coupled plasma atomic emission spectroscopy. The N_2 adsorption-desorption isotherms under static conditions were obtained by using automatic volumetric vapor adsorption measurement called BELSORP-max. Transmission electron microscopy (JEM 1400 Plus operating at 120 kV, JEM 2100 Plus operating at 200 kV, and JEM F200 EDS operating at 200 kV) and scanning electron microscopy (JSM-7800F Prime), were used for structural characterizations. Thermogravimetric analysis (TGA) experiments were performed on a PerkinElmer TGA 8000 in an O_2 environment with a temperature ramping rate of 20 ℃/min.

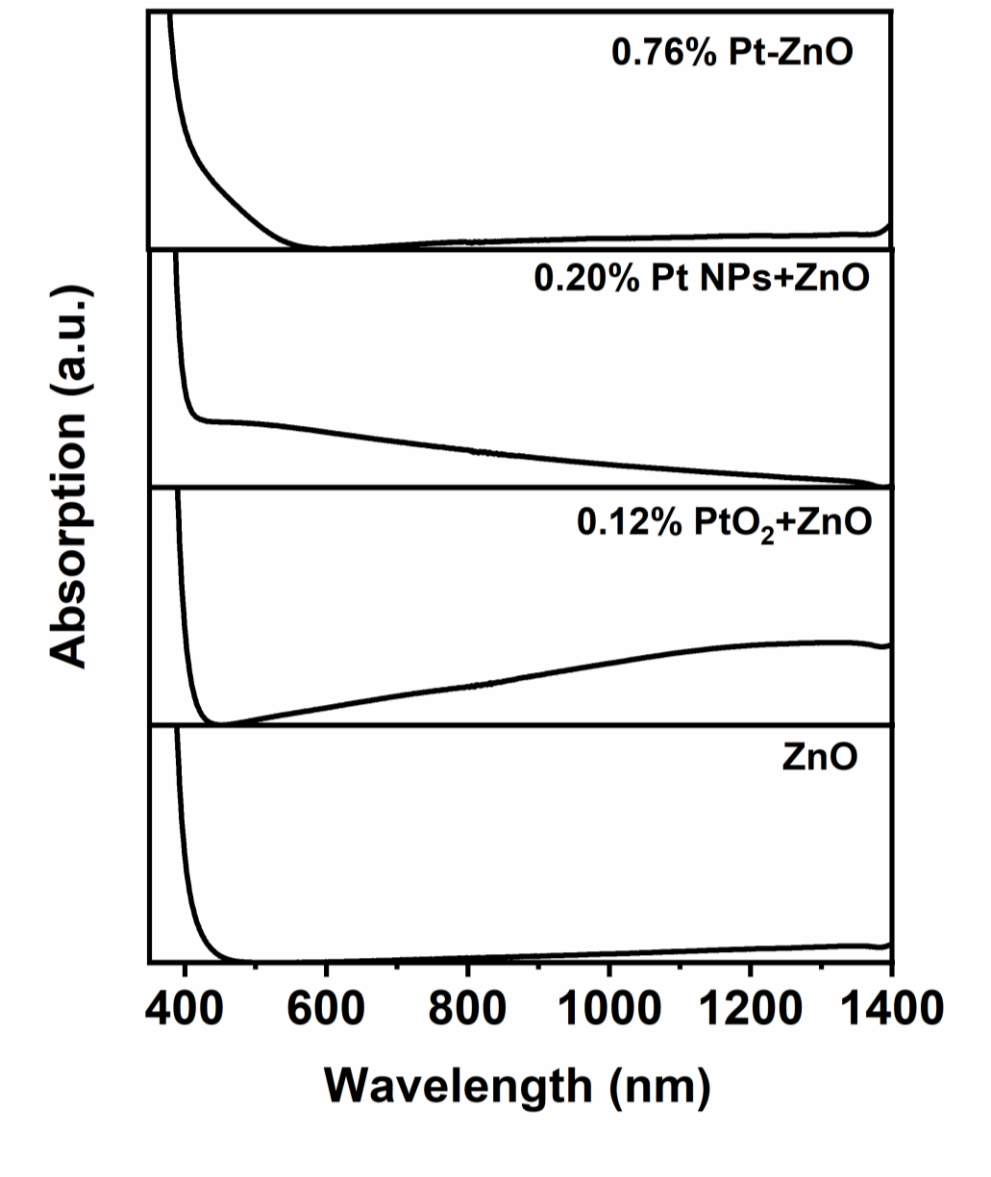

Figure S1. UV-Vis spectra of Pt-ZnO, mixture of Pt NPs and ZnO (Pt NPs+ZnO), mixture of PtO_2 and ZnO (PtO_2+ZnO), and ZnO, respectively. A sharp absorption edge around 380 nm was observed in pure ZnO sample, agreeing well with the bandgap of ZnO (~3.26 eV) at room temperature. A weak shoulder absorption signal was observed around 400-500 nm for the Pt-ZnO sample. The incorporation of Pt into the host lattice of Zn not only reconstructed the energy band of ZnO, but also brought plenty of tail states near the conduction band minimum (CBM) and valence band maximum (VBM). In contrast, if Pt and PtO_2 were added into ZnO as a physical mixture, different UV-Vis spectra were observed.

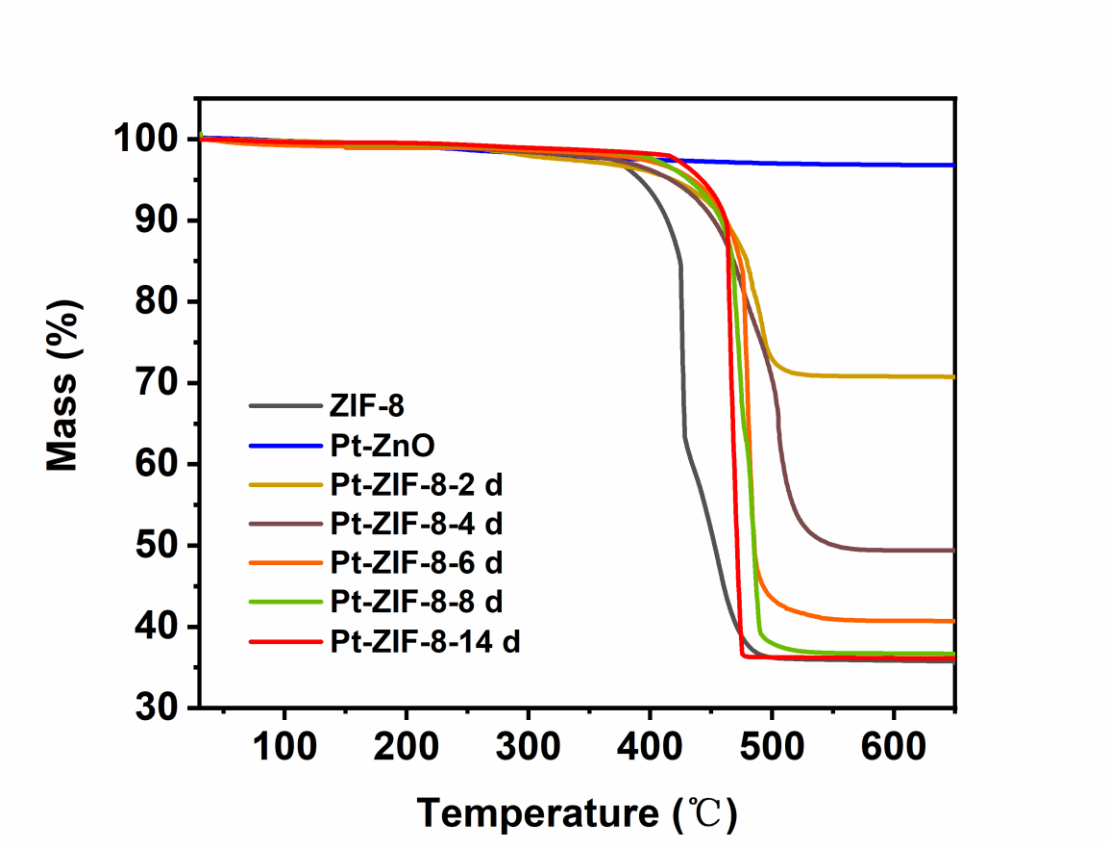

Figure S2. TGA curves of Pt-ZIF-8 synthesized for reaction time at 140 ℃. All measurements data were collected under flowing oxygen using a temperature ramp rate of 20 ℃·min^{-1}.

Table S1. Conversion yields of Pt-ZIF-8 at the different reaction time.

Sample	Conversion (%)
Pt-ZIF-8-2 d	23.15
Pt-ZIF-8-4 d	57.25
Pt-ZIF-8-6 d	81.03
Pt-ZIF-8-CVD (8 d)	96.03
Pt-ZIF-8-14 d	98.29

TGA was performed in O_2 environment to estimate the conversion rate of ZnO to ZIF-8. ZIF-8 decomposed completely to ZnO when temperature exceeds 500 ℃ in O_2. Therefore, the CVD conversion yield could be calculated using the following formula:

$$\text{Conv. (\%)} = \frac{m_{loss}/(M_{ZIF-8} - M_{ZnO})}{m/Mr_{ZnO}}$$

m_{loss}: the weight loss from ZIF-8 to ZnO measured by TGA;

m: the residual weight after complete decomposition in O_2.

$M_{ZIF\text{-}8}$ and M_{ZnO} are the molar masses of ZIF-8 and ZnO, respectively.

The conversion rates of doped ZnO to doped ZIF-8 can be estimated similarly. A summary of conversion yield was listed below.

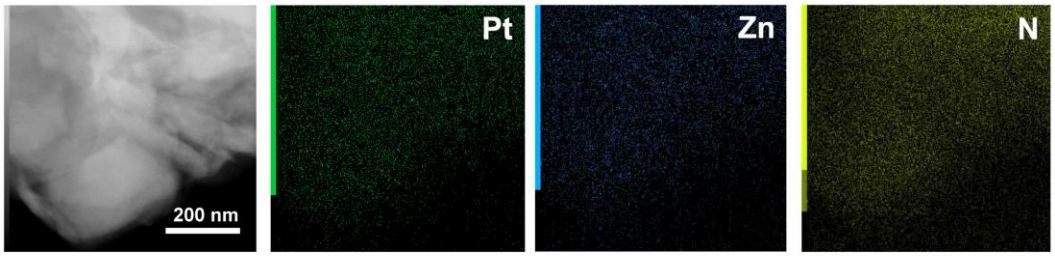

Figure S3. EDS mapping images of Pt-ZIF-8-CVD: Pt (green), Zn (blue), and N (yellow).

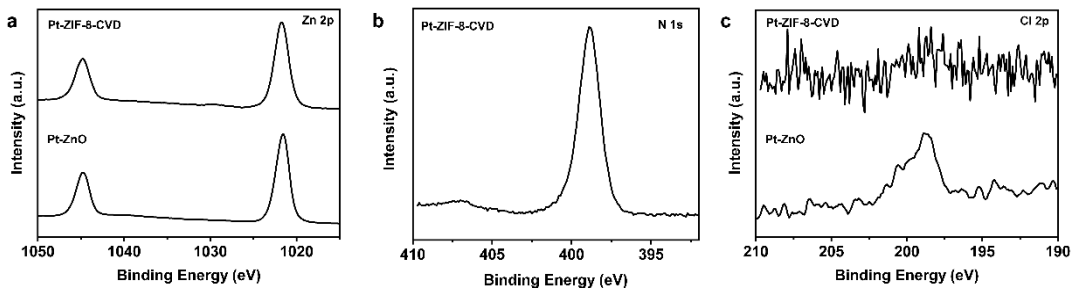

Figure S4. XPS spectra for Pt-ZnO and Pt-ZIF-8-CVD. **(a)** Zn 2p spectra of Pt-ZnO (1021.5 eV and 1044.5 eV) and Pt-ZIF-8-CVD (1021.8 eV and 1044.8 eV), **(b)** N 1s spectrum and **(c)** Cl 2p spectra. After CVD conversion, the binding energy of Zn 2p moved to slightly higher values. There was a minor Cl 2p peak in the as-synthesized Pt-ZnO, possibly due to unreacted Pt salts absorbed on the surface.

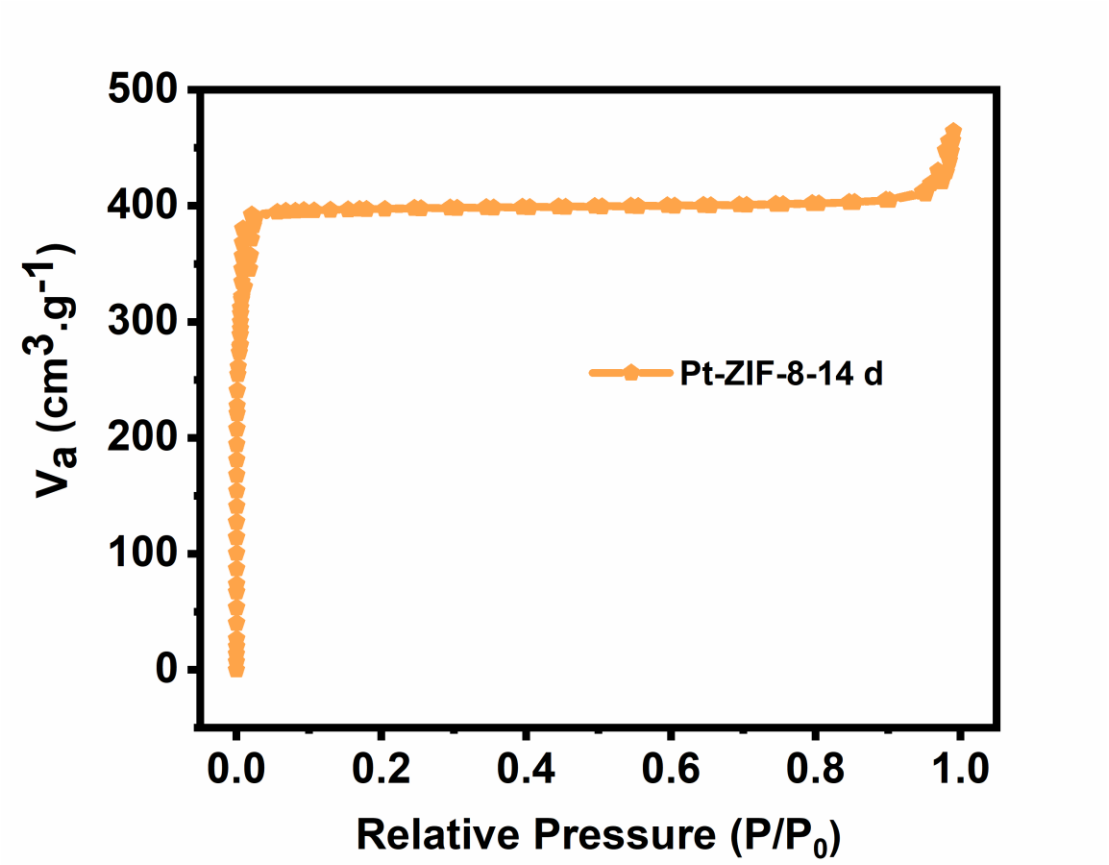

Figure S5. Nitrogen sorption isotherms of Pt-ZIF-8-14 d, showing Pt-ZIF-8-14 d could remain framework of ZIF-8 with good structural integrity.

Table S2. N_2 adsorbed capacities and BET surfaces of C-ZIF-8, Pt-ZIF-8-CVD and Pt-ZIF-8-14 d.

Sample	N_2 Adsorbed Capacity (cc/g)	BET Surface (m^2/g)
C-ZIF-8	400	1275
Pt-ZIF-8-CVD	407	1286
Pt-ZIF-8-14 d	404	1260

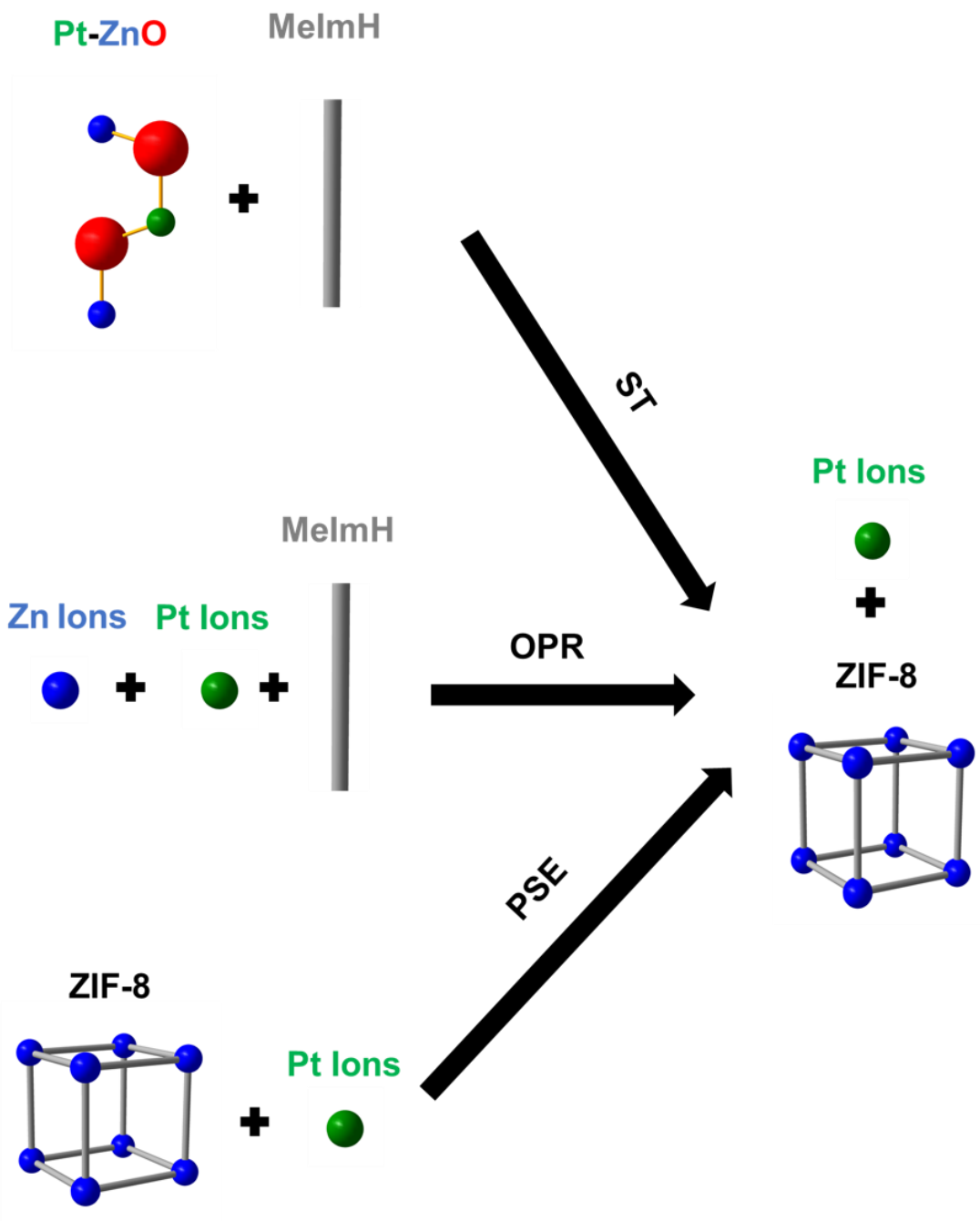

Figure S6. A brief schematic to shown various solution-phase synthesis routes to prepare Pt/ZIF-8.

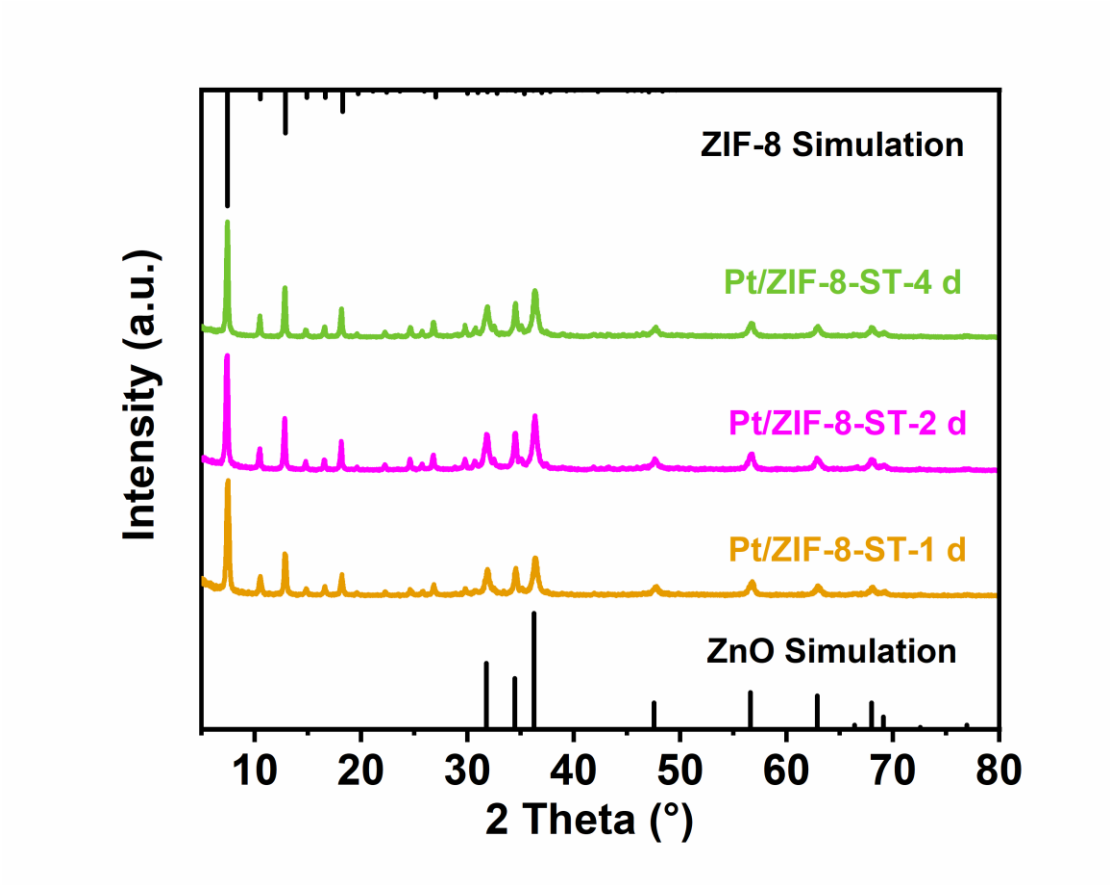

Figure S7. PXRD patterns of Pt/ZIF-8-ST obtained with different reaction time by solvent transformation (ST). Pt-ZnO were converted for 1 d (orange, Pt/ZIF-8-ST-1d), 2 d (purple, Pt/ZIF-8-ST-2d) and 4 d (green, Pt/ZIF-8-ST-4d), respectively.

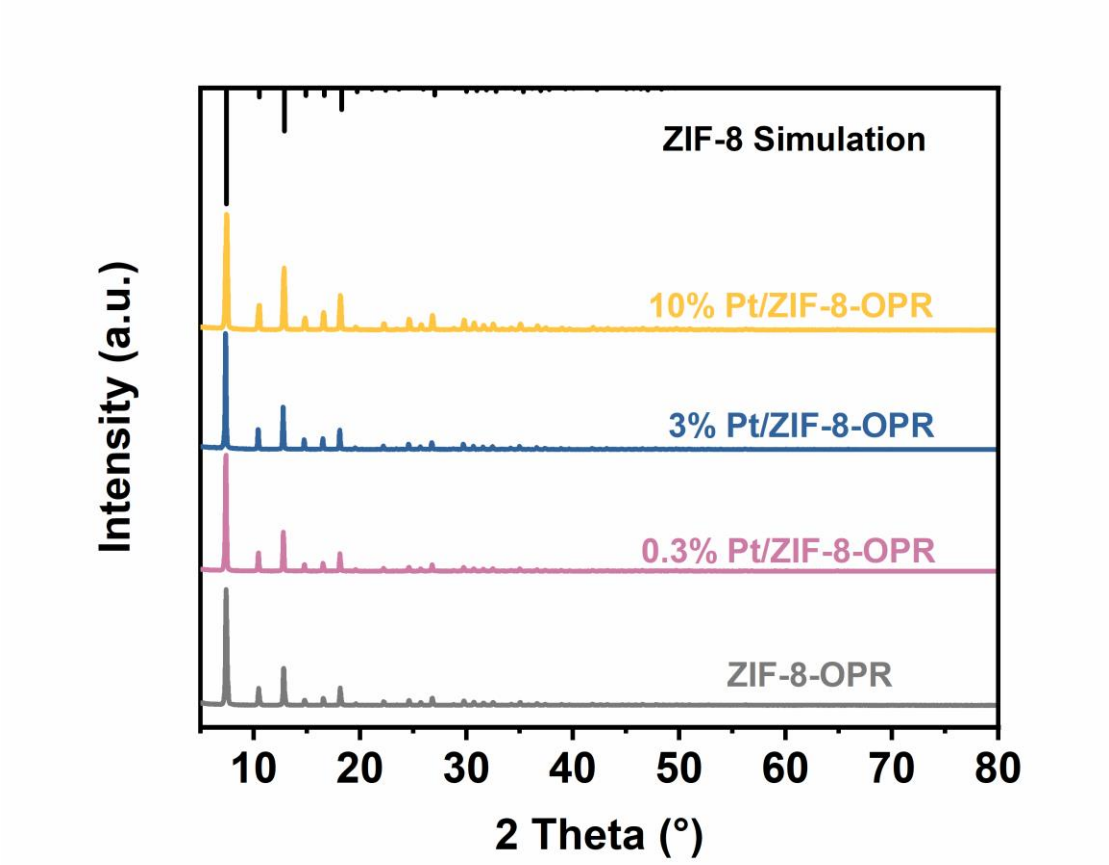

Figure S8. PXRD patterns of Pt/ZIF-8-OPR with different Pt feed. Samples were synthesized with 0 % (gray, ZIF-8-OPR), 0.3 % (purple, 0.3% Pt/ZIF-8-OPR), 3 % (blue, 3% Pt/ZIF-8-OPR) and 10 % (orange, 10% Pt/ZIF-8-OPR) Pt feed respectively. PXRD analysis showed that the Pt/ZIF-8-OPR samples displayed the characteristic peaks of ZIF-8.

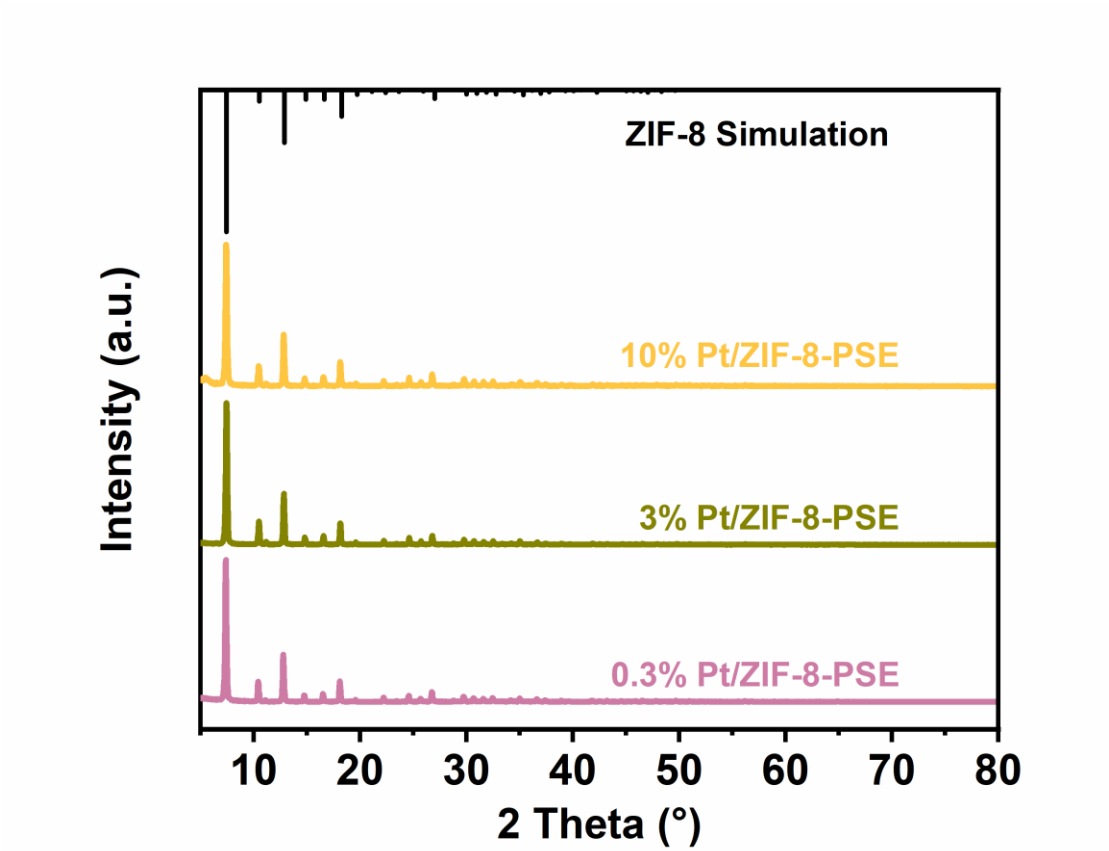

Figure S9. PXRD patterns of Pt/ZIF-8-PSE with different Pt feed. Samples were synthesized with 0.3% (purple, 0.3% Pt/ZIF-8-PSE), 3% (olive, 3% Pt/ZIF-8-PSE) and 10% (orange, 10% Pt/ZIF-8-PSE) Pt feed respectively. PXRD analysis showed that the Pt/ZIF-8-PSE samples displayed the characteristic peaks of ZIF-8.

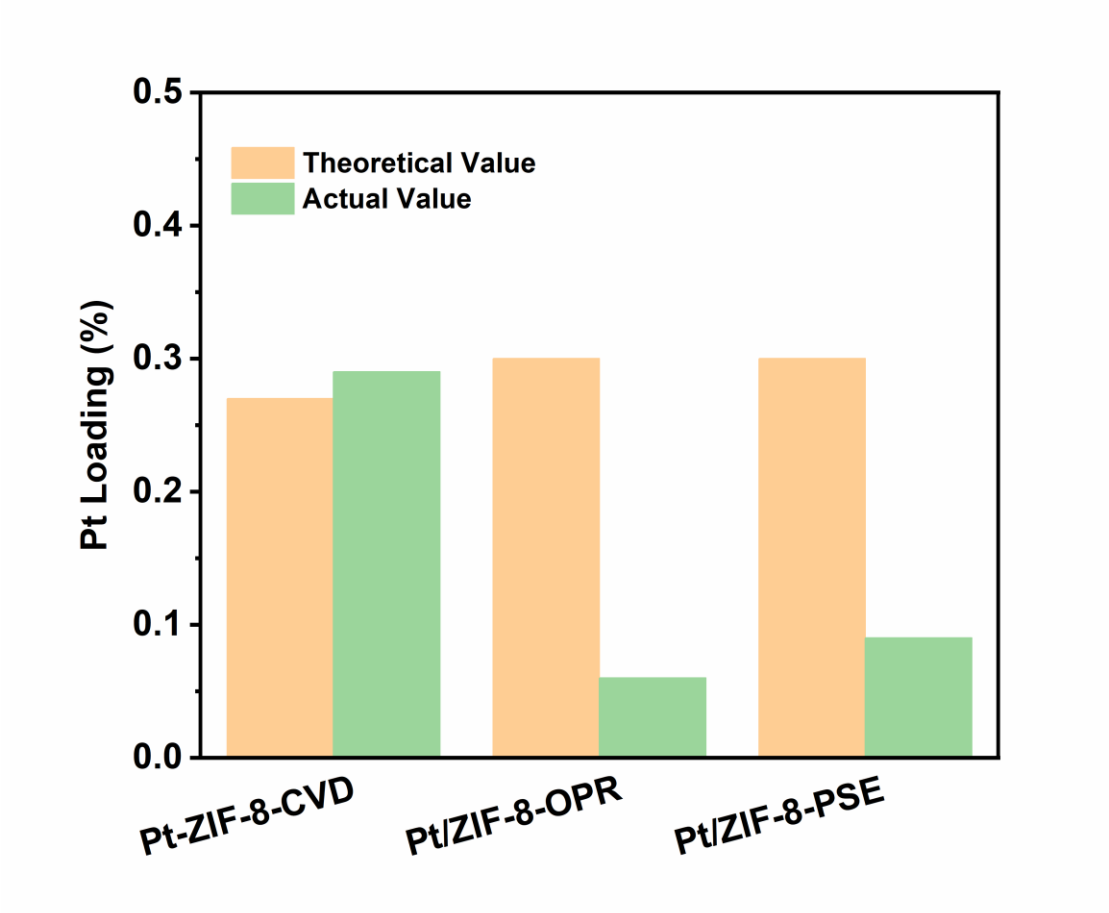

Figure S10. Comparison of Pt theoretical and actual loading of Pt/ZIF-8-CVD, 0.3% Pt/ZIF-8-OPR and 0.3% Pt/ZIF-8-PSE. The theoretical loading of Pt was calculated based on the Pt: Zn ratio in the starting materials. The actual loading of Pt was calculated based on ICP measurement when Pt/ZIF-8-CVD, 0.3% Pt/ZIF-8-OPR and 0.3% Pt/ZIF-8-PSE were completely dissolved.

Table S3. Pt theoretical and actual loading of Pt-ZIF-8-CVD, Pt/ZIF-8-OPR and Pt/ZIF-8-PSE.

Sample	Theoretical Value	Actual Value
Pt-ZIF-8-CVD	0.27 %	0.29 %
Pt/ZIF-8-OPR	0.30 %	0.06 %
	3.00 %	0.18 %
	10.00 %	0.45 %
Pt/ZIF-8-PSE	0.30 %	0.09 %
	3.00 %	1.23 %
	10.00 %	3.57 %

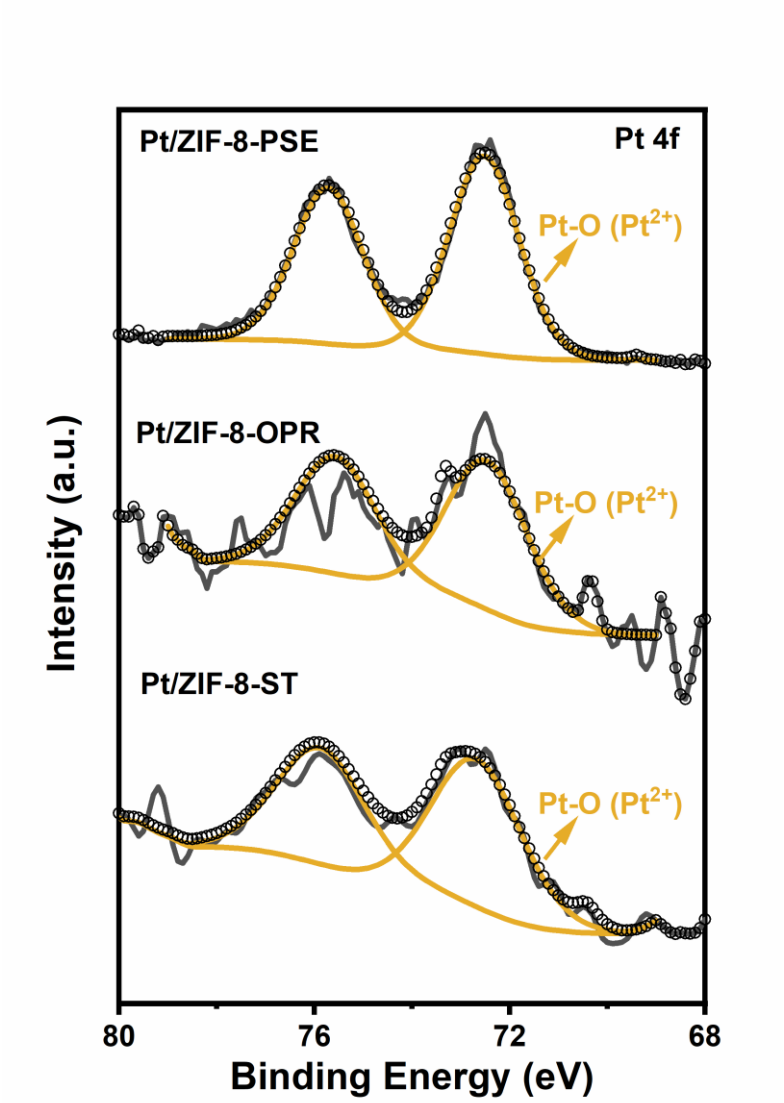

Figure S11. XPS characterizations of Pt/ZIF-8-ST, Pt/ZIF-8-OPR, and Pt/ZIF-8-PSE, respectively. Pt/ZIF-8-ST was formed through hydrothermal transformation of Pt-ZnO. The peaks around 72.7 eV and 75.9 eV which assigned to Pt^{2+} $4f_{7/2}$, which remained unchanged compared to that of Pt-ZnO. This might indicate a similar oxygen coordination environment before and after the hydrothermal conversion. Similarly, the main peaks of Pt/ZIF-8-OPR (72.5 eV and 75.6 eV) and Pt/ZIF-8-PSE (72.5 eV and 75.7 eV) also agreed well with vale for Pt^{2+} $4f_{7/2}$ in commercial PtO_2 (Fig. S12, ESI†).

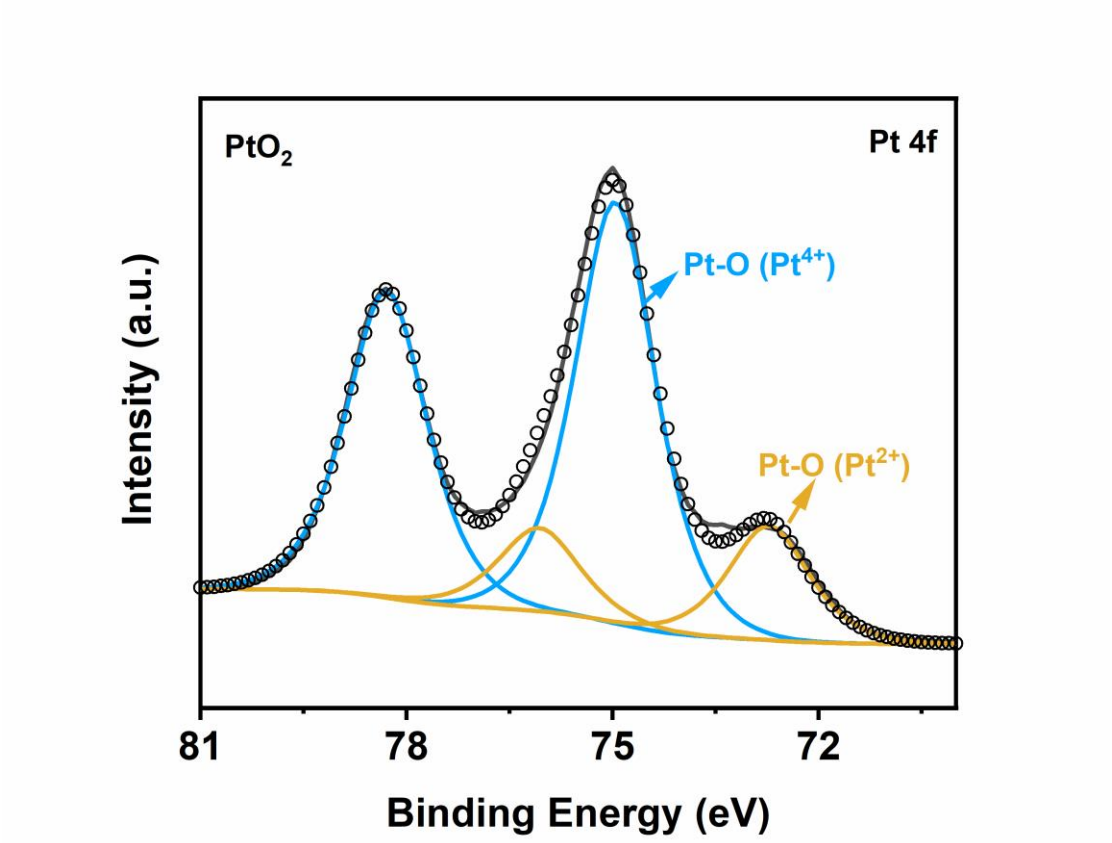

Figure S12. XPS spectrum of commercial PtO_2. (Pt^{2+}: 72.7 eV and 76.0 eV; Pt^{4+}: 75.0 eV and 78.3 eV)

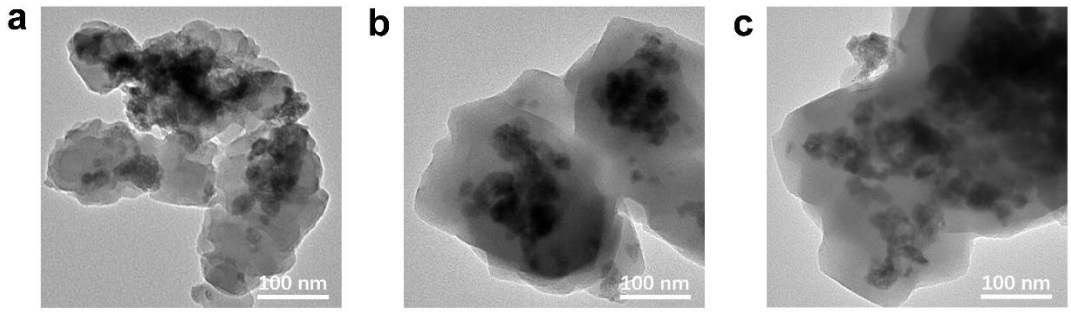

Figure S13. TEM images of **(a)** Pt/ZIF-8-ST-1 d, **(b)** Pt/ZIF-8-ST-2 d **(c)** and Pt/ZIF-8-ST-4 d.

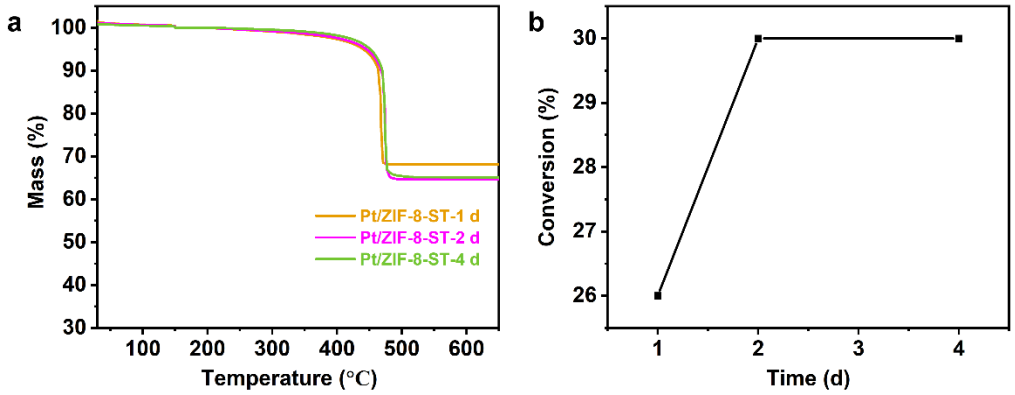

Figure S14. Conversion yield of Pt/ZIF-8-ST estimated by the TGA curve.(a) TGA plots of Pt/ZIF-8-ST with different reaction time by solvent transformation. All measurements data were collected under flowing oxygen using a temperature ramp of 20 °C·min^{-1}. **(b)** Conversion yield of Pt/ZIF-8-ST. Solvent transformation method could partially convert Pt-ZnO to Pt/ZIF-8, as shown in both PXRD and TEM analysis. In addtion, TGA anslysis showed the conversion yield of Pt/ZIF-8-ST-2 d and Pt/ZIF-8-ST-4 d was closed to each other, possibly because the generated ZIF-8 on the surface of Pt-ZnO would hinder the diffusion solvated organic linkers. The conversion yield reached a plateau at around 30%. Further extending reaction time beyond 2 days couldn't increase the conversion yield.

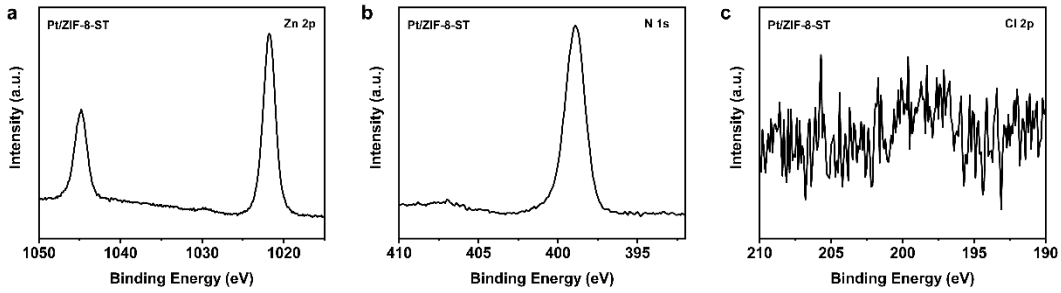

Figure S15. XPS spectra for Pt/ZIF-8-ST of **(a)** Zn 2p spectrum (1021.8 eV and 1044.8 eV), **(b)** N 1s spectrum and **(c)** Cl 2p spectrum.When Pt-ZnO was converted to Pt/ZIF-8-ST in solution, Zn $2p_{7/2}$ peaks shifted slightly from 1021.5 eV to 1021.8 eV.

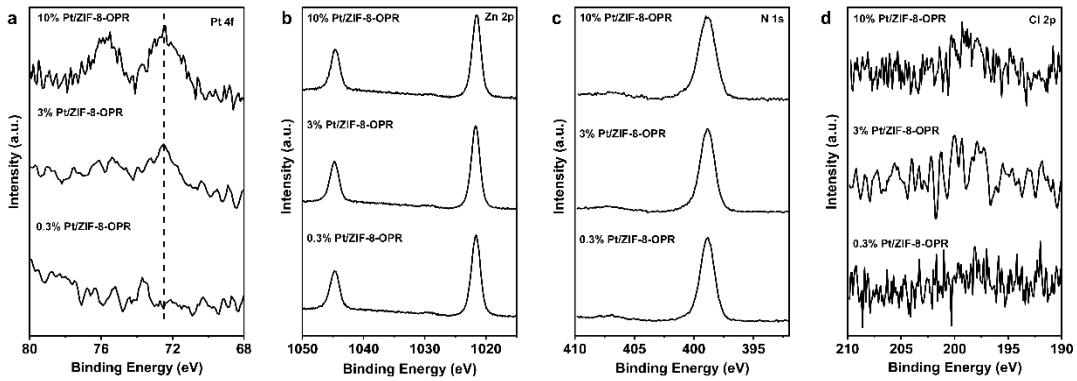

Figure S16. XPS spectra of 0.3% Pt/ZIF-8-OPR, 3% Pt/ZIF-8-OPR and 10% Pt/ZIF-8-OPR. **(a)** Pt 4f spectra, **(b)** Zn 2p spectra, **(c)** N 1s spectra, and **(d)** Cl 2p spectra.

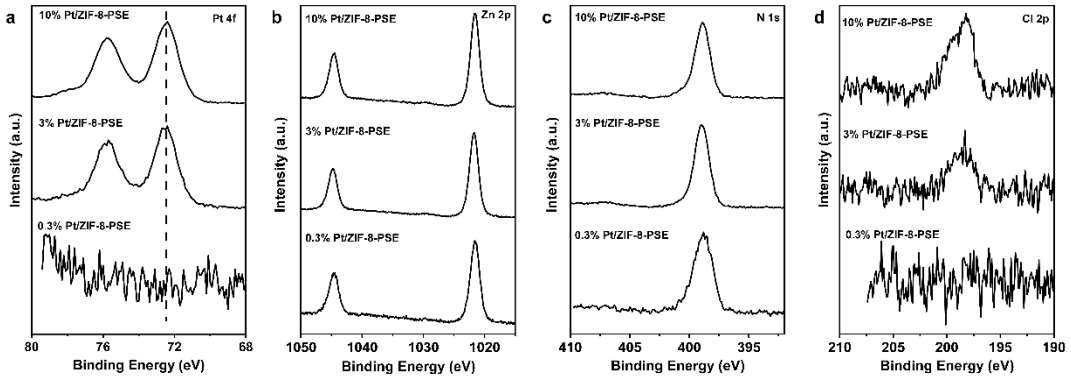

Figure S17. XPS spectra of 0.3% Pt/ZIF-8-PSE, 3% Pt/ZIF-8-PSE and 10% Pt/ZIF-8-PSE . **(a)** Pt 4f spectra, **(b)** Zn 2p spectra, **(c)** N 1s spectra, and **(d)** Cl 2p spectra.

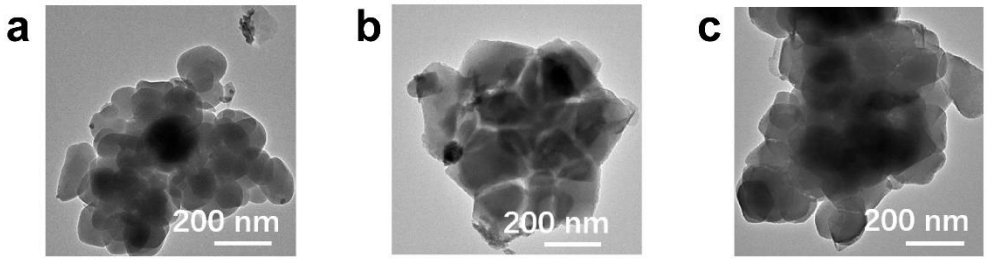

Figure S18. TEM images of Pt/ZIF-8-PSE with different Pt feed: **(a)** 0.3% Pt/ZIF-8-PSE, **(b)** 3% Pt/ZIF-8-PSE and **(c)** 10% Pt/ZIF-8-PSE. TEM images showed there were some nanoparticles outside the ZIF-8.

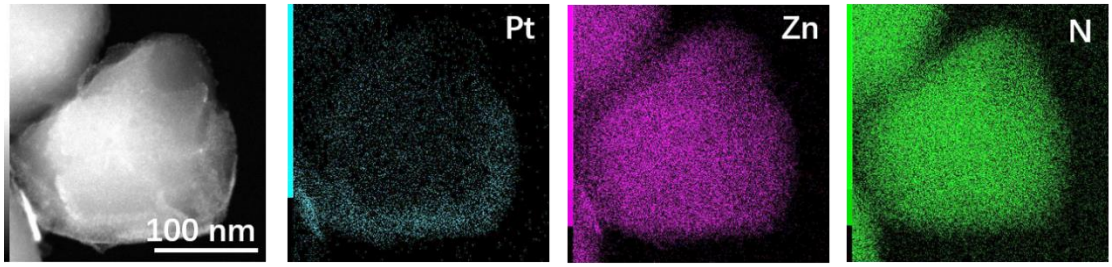

Figure S19. EDS mapping images of 3% Pt/ZIF-8-PSE. The Zn and N in EDS mapping of 3% Pt/ZIF-8-PSE were uniformly dispersed, while there was more Pt on the outside than on the inside

Table S4. Pt-ZIF-8 conversion yields under different reaction conditions.

Sample	Conversion (%)
Pt-ZIF-8-6 h-Air	12.64
Pt-ZIF-8-6 h-H_2O	8.24
Pt-ZIF-8-6 h-N_2	12.56
Pt-ZIF-8-6 h-Vacuum	12.56

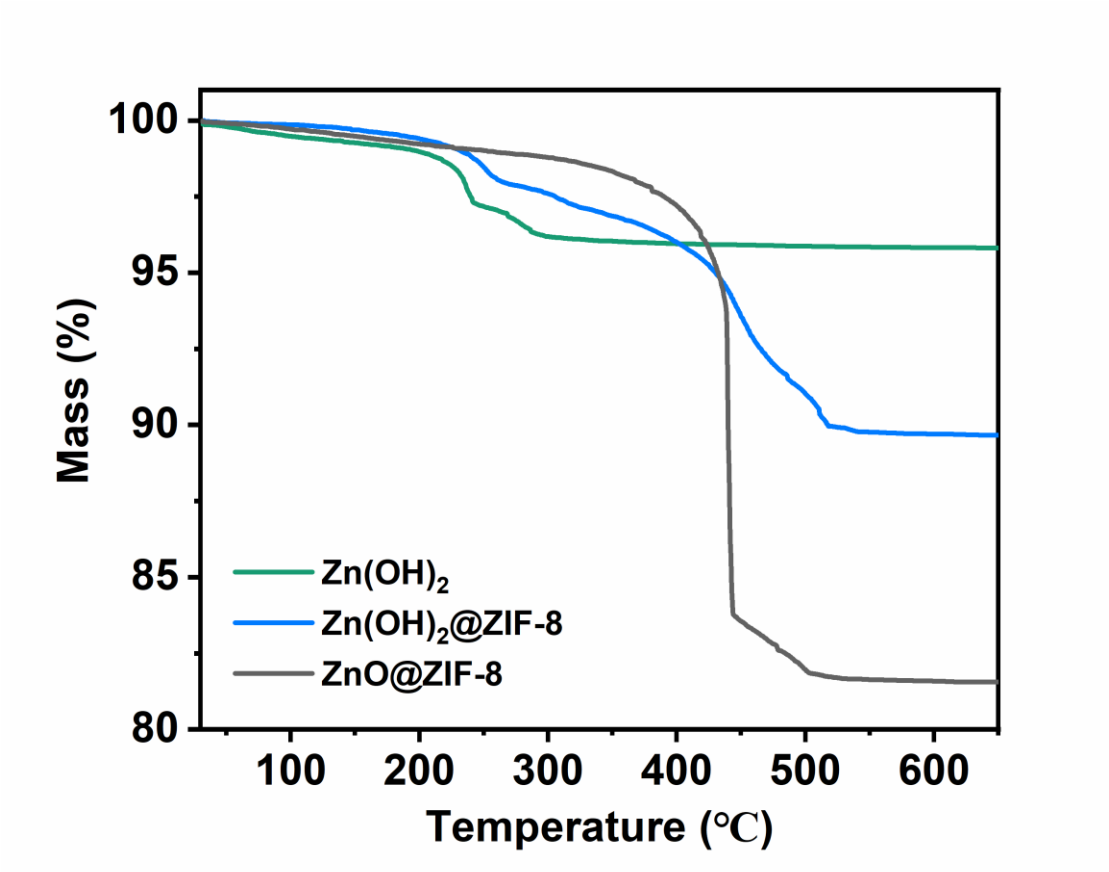

Figure S20. TGA plots of ZIF-8 under the different humidity. ZIF-8 samples were transformed from $Zn(OH)_2$ and ZnO respectively with different H_2O addition volume to investigate the influence of H_2O during the transformation.

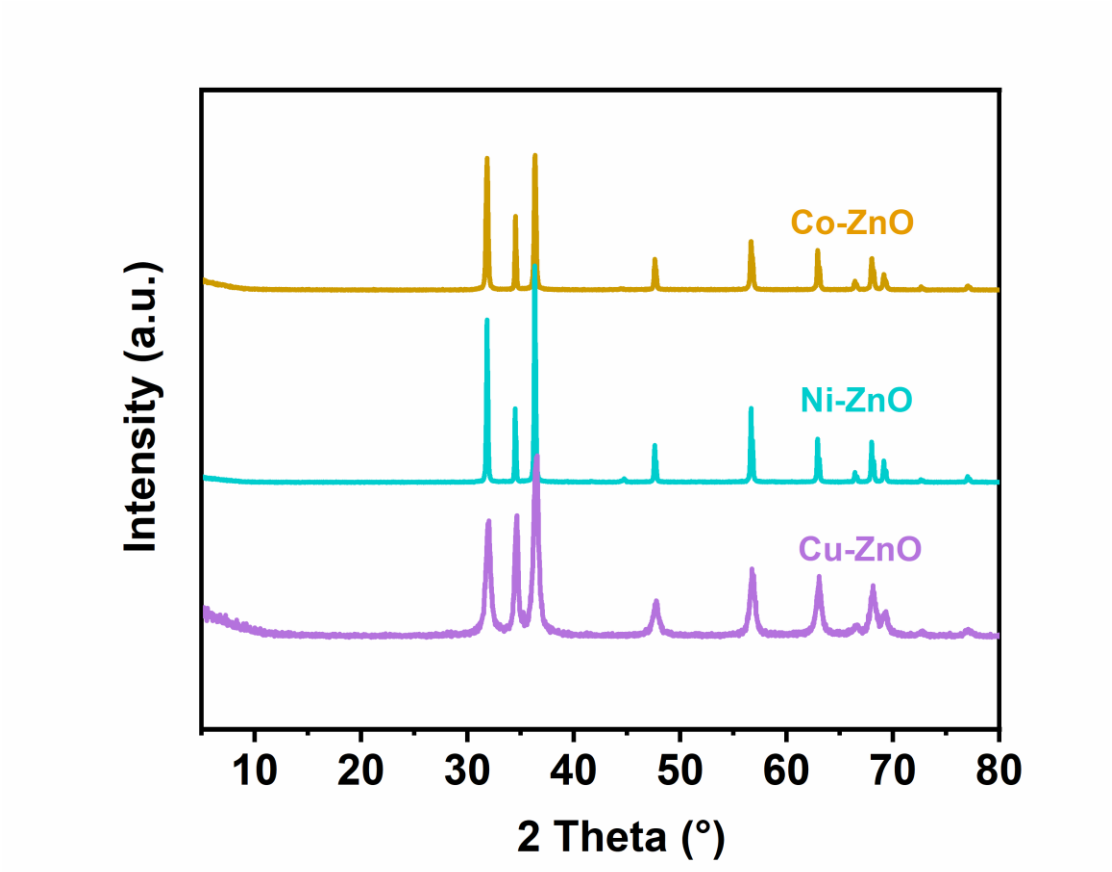

Figure S21. PXRD patterns of Cu doped ZnO (purple, Cu-ZnO), Ni doped ZnO (aqua, Ni-ZnO) and Co doped ZnO (gold, Co-ZnO) respectively. PXRD analysis showed that the samples displayed the characteristic peaks of ZnO.

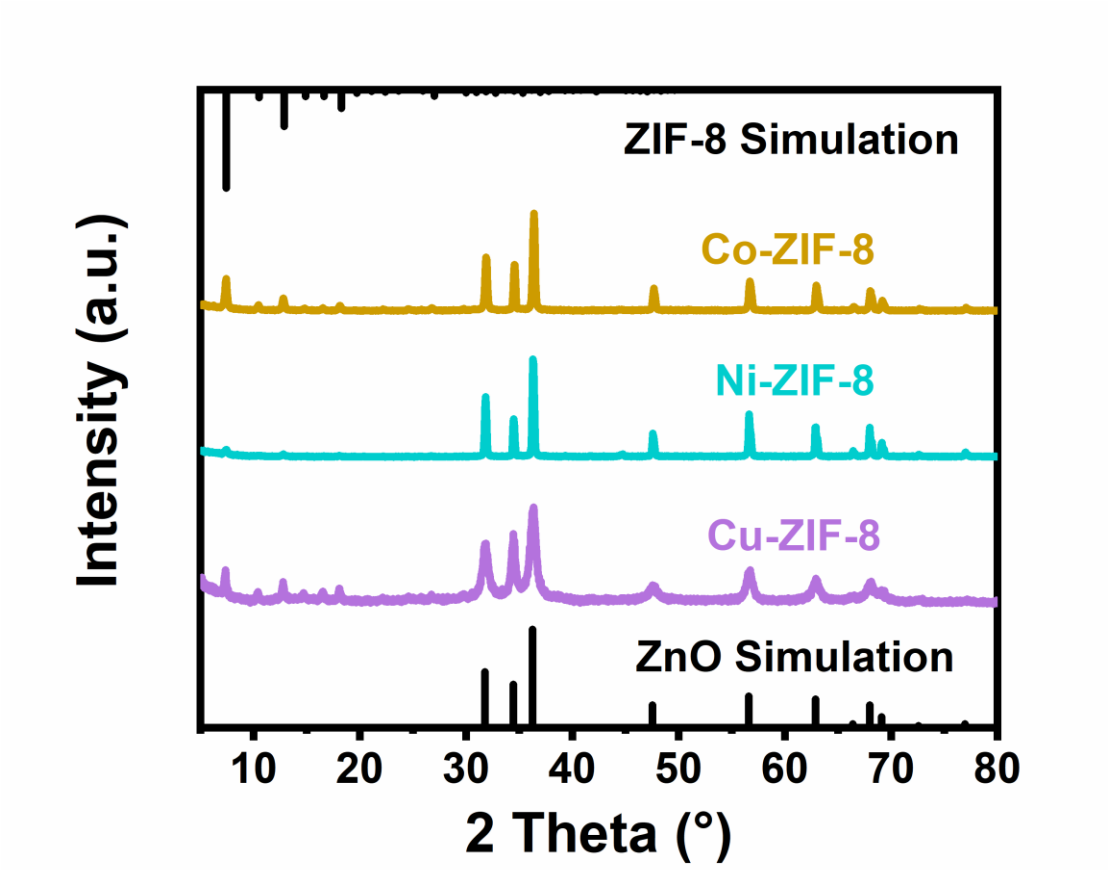

Figure S22. PXRD patterns of Co-ZIF-8, Ni-ZIF-8, Cu-ZIF-8, simulated ZnO, and simulated ZIF-8. All samples showed obvious peaks of ZIF-8 after vapor conversion.

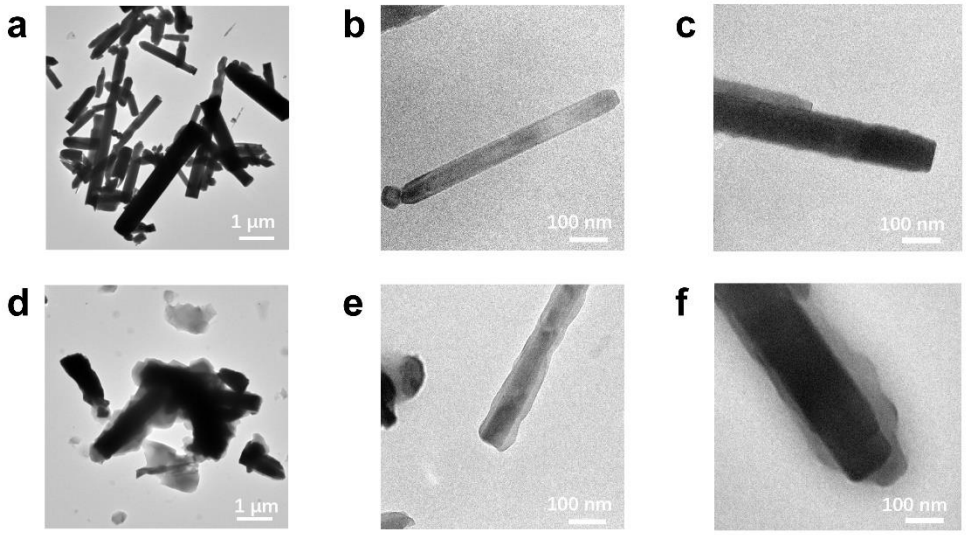

Figure S23. TEM images of M-ZnO and M-ZIF-8 (M=Cu, Co, Ni). **(a)** Cu-ZnO, **(b)** Co-ZnO, **(c)** Ni-ZnO, **(d)** Cu-ZIF-8, **(e)** Co-ZIF-8, and **(f)** Ni-ZIF-8.

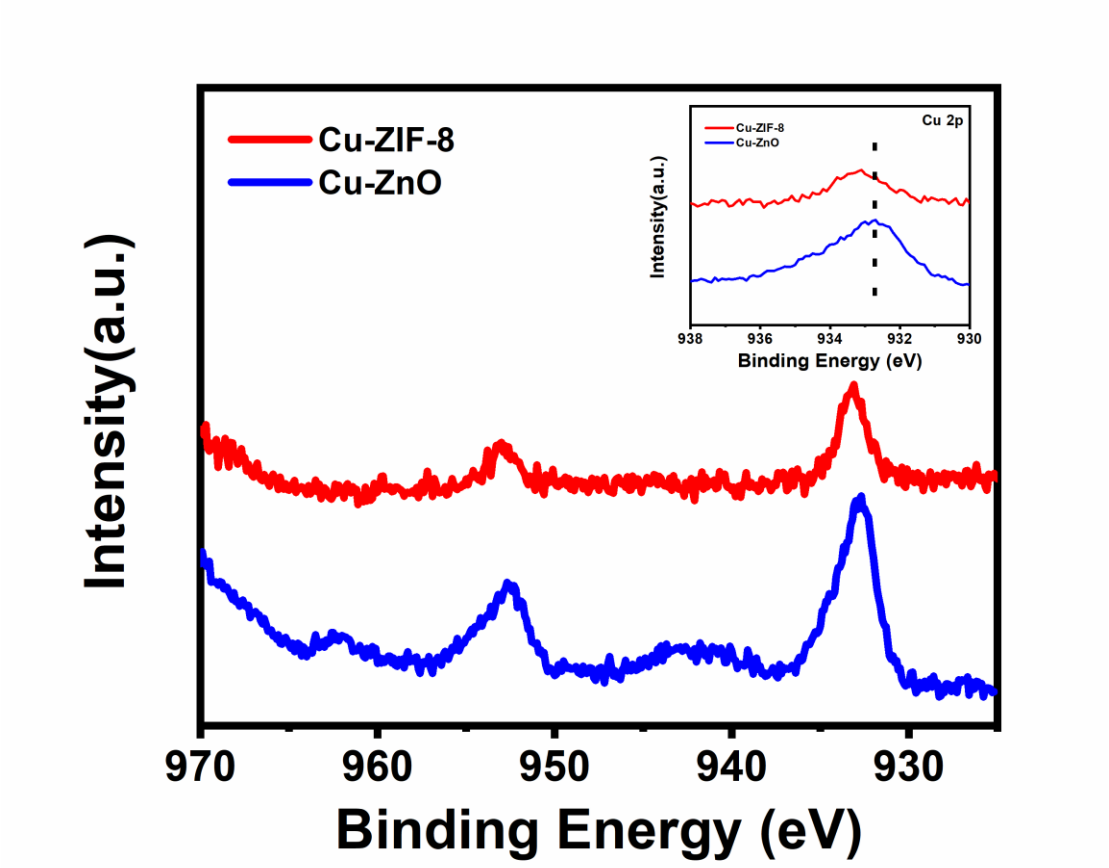

Figure S24. XPS spectra of Cu-ZnO and Cu-ZIF-8.

XPS characterizations were also performed to understand the chemical environment for the metal dopants. The peaks around 932.7 eV were assigned to Cu2+ in Cu-ZnO, lower than the peak around 933.1 eV in Cu-ZIF-8. Besides, the satellite peak assigning to Cu2+ disappeared after CVD conversion. These results could be ascribed to the monodispersed Cu in ZIF-8. Interestingly, similar results were also found in Co-ZIF-8 and Ni-ZIF-8 (Figs. S25 and 26, ESI†).

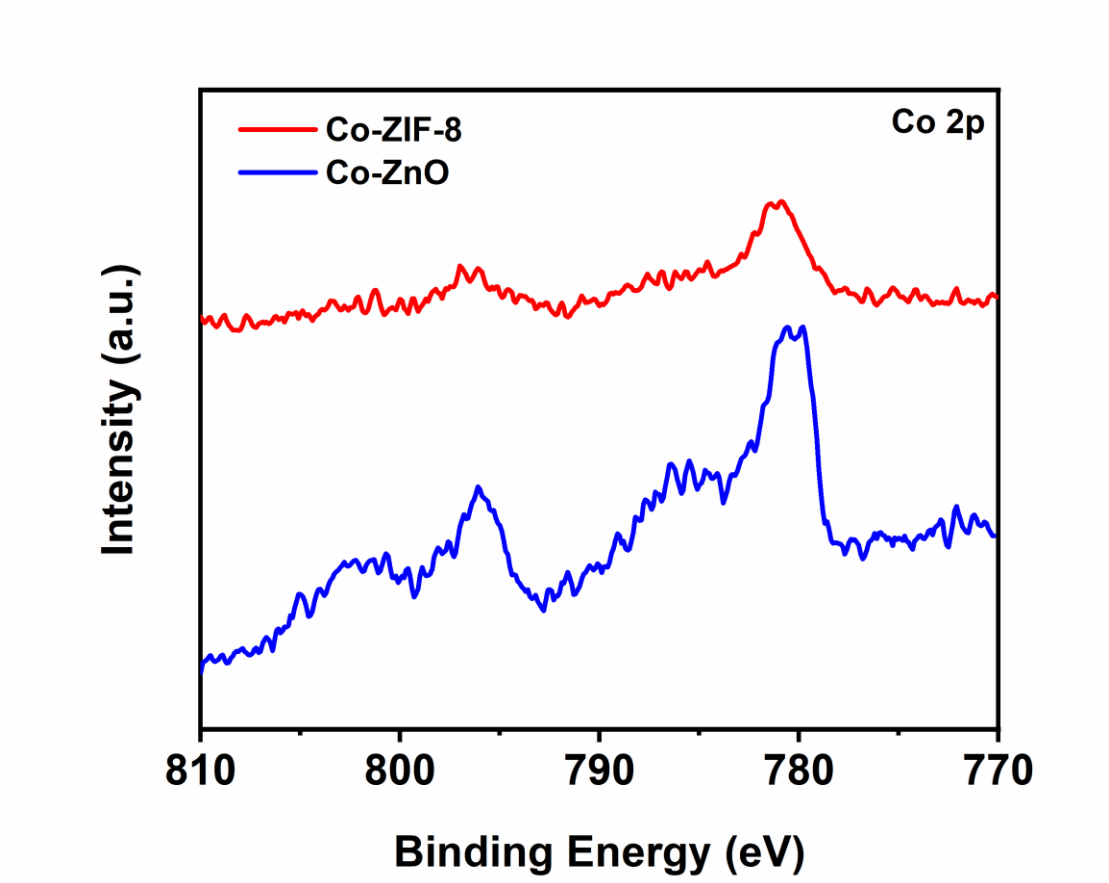

Figure S25. Co 2p XPS spectra of Co-ZnO and Co-ZIF-8.

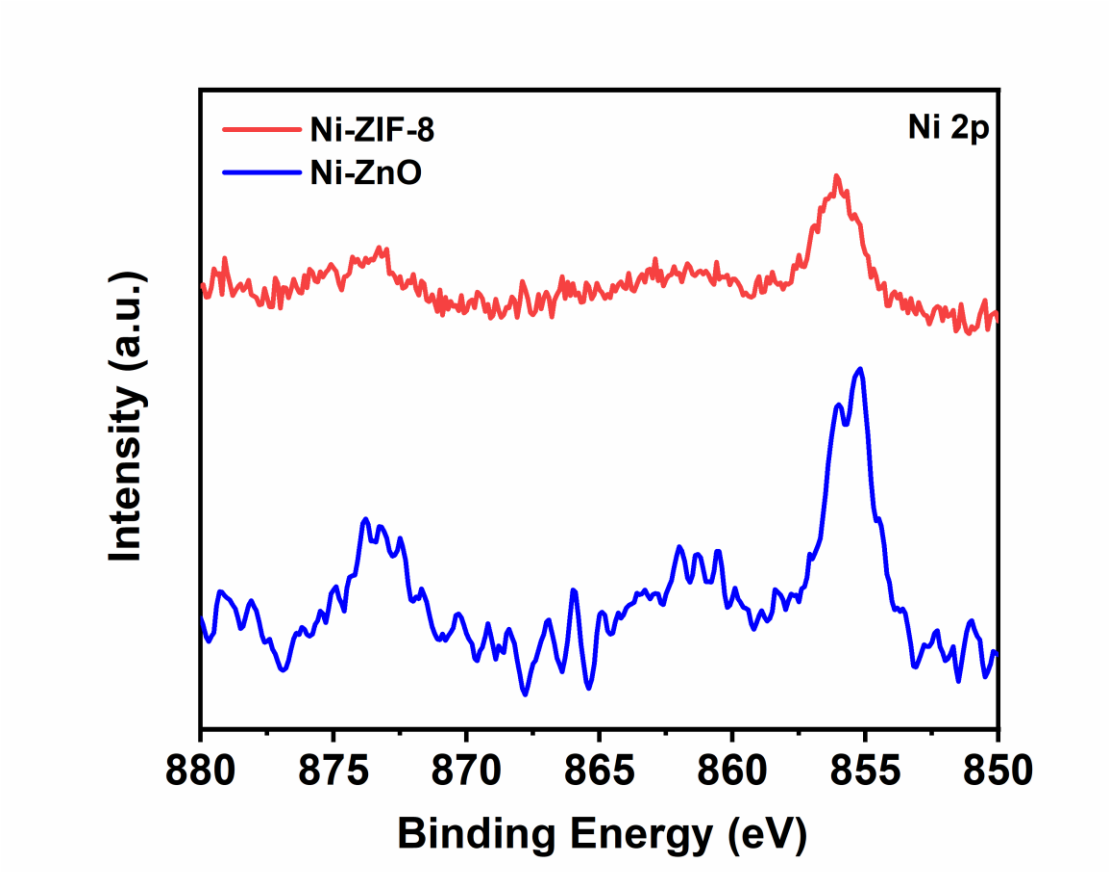

Figure S26. Ni 2p XPS spectra of Ni-ZnO and Ni-ZIF-8.

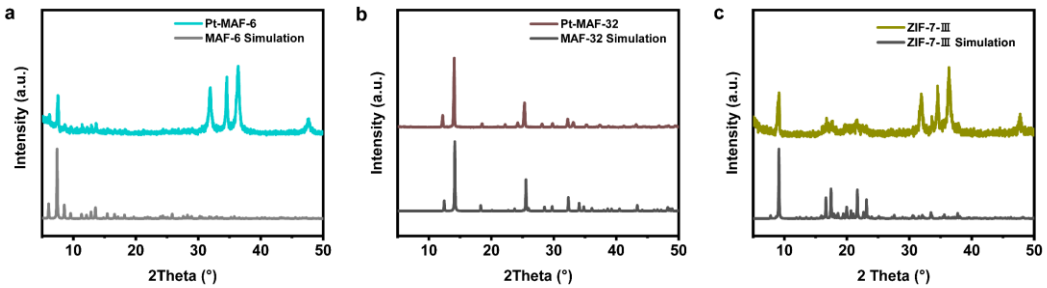

Figure S27. PXRD of Pt-ZIFs synthesized through solvent-free approach.

We used 2-ethylimidazole and benzimidazole to convert Pt-ZnO to Pt-MAF-6, Pt-MAF-32, and Pt-ZIF-7-III. A slightly different range of temperatures was carefully selected for the conversion reaction to prepare different MMOFs.

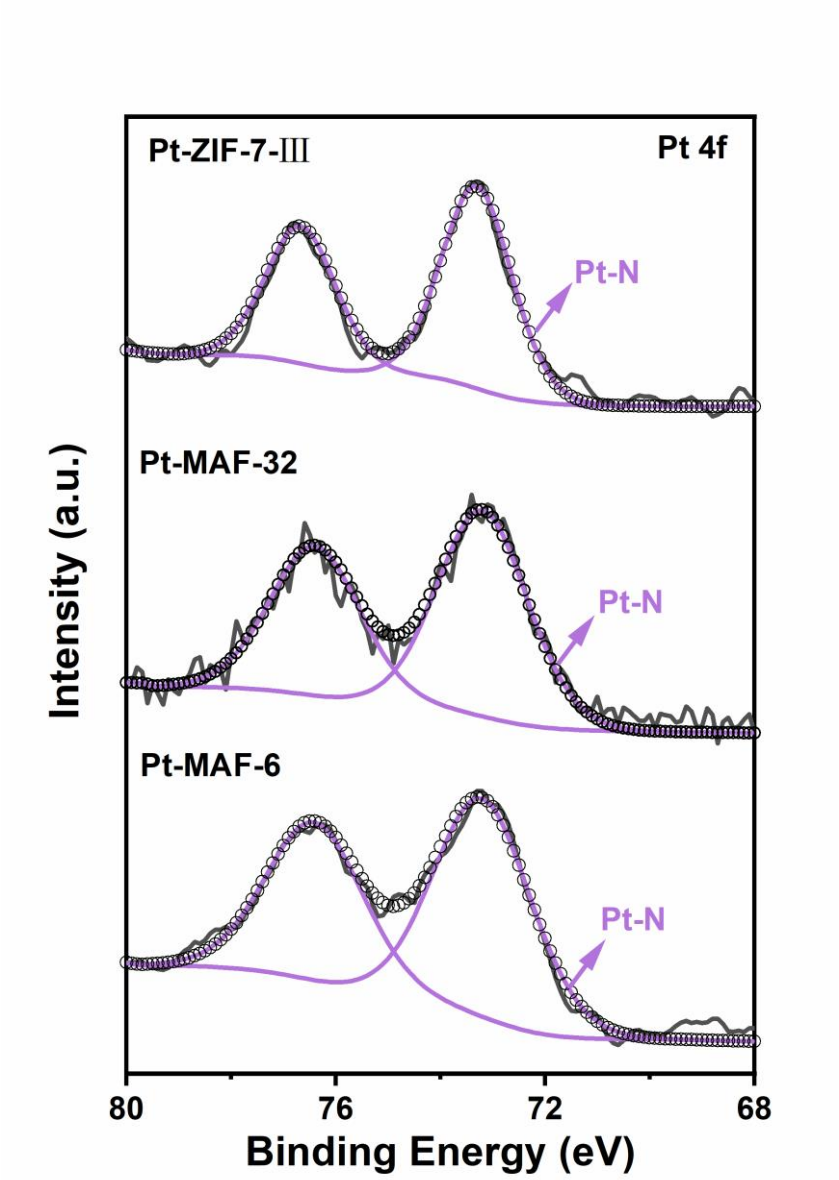

Figure S28. XPS spectra of Pt-ZIFs with different organic ligands synthesized using a solvent-free approach: Pt-MAF-6 (73.20 eV), Pt-MAF-32 (73.19 eV), and Pt-ZIF-7-III (73.30 eV).

XPS characterization was performed for solvent-free converted Pt-ZIFs. All samples showed a pair of symmetrical Pt 4f peaks around 73.3 eV and 76.7 eV, similar to that of Pt-ZIF-8-CVD and Pt-N_4 sites in a previous report. It's important to note all the organic linkers used in this work formed tetrahedral metal-nitrogen coordination in the corresponding ZIFs, therefore sharing a similar chemical environment for Pt.